



Article

pubs.acs.org/Biomac[Terms of Use](#)

Antigen Delivery by Lipid-Enveloped PLGA Microparticle Vaccines Mediated by *in Situ* Vesicle Shedding

Melissa C. Hanson,[†] Anna Bershteyn,[‡] Monica P. Crespo,^{§,⊥} and Darrell J. Irvine^{*,†,‡,||,#,○}

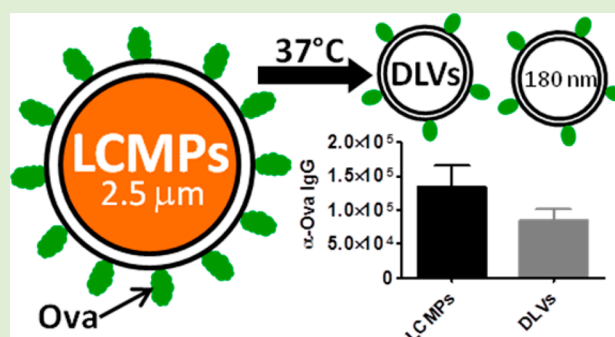
[†]Department of Biological Engineering, [‡]Department of Materials Science and Engineering, [§]Health Sciences and Technology Program, and ^{||}David H. Koch Institute for Integrative Cancer Research, Massachusetts Institute of Technology, 77 Massachusetts Avenue, Cambridge, Massachusetts 02139, United States

[⊥]Harvard Medical School, 25 Shattuck Street, Boston, Massachusetts 02115, United States

[#]The Ragon Institute of MGH, MIT, and Harvard, 400 Technology Square, Cambridge, Massachusetts 02139, United States

[○]Howard Hughes Medical Institute, 4000 Jones Bridge Road, Chevy Chase, Maryland 20815, United States

ABSTRACT: Lipid-coated poly(lactide-*co*-glycolide) microparticles (LCMPs) consist of a solid polymer core wrapped by a surface lipid bilayer. Previous studies demonstrated that immunization with LCMPs surface-decorated with nanograms of antigen elicit potent humoral immune responses in mice. However, the mechanism of action for these vaccines remained unclear, as LCMPs are too large to drain efficiently to lymph nodes from the vaccination site. Here, we characterized the stability of the lipid envelope of LCMPs and discovered that in the presence of serum the lipid coating of the particles spontaneously delaminates, shedding antigen-displaying vesicles. Lipid delamination generated 180 nm liposomes in a temperature- and lipid/serum-dependent manner. Vesicle shedding was restricted by inclusion of high- T_M lipids or cholesterol in the LCMP coating. Administration of LCMPs bearing stabilized lipid envelopes generated weaker antibody responses than those of shedding-competent LCMPs, suggesting that *in situ* release of antigen-loaded vesicles plays a key role in the remarkable potency of LCMPs as vaccine adjuvants.



INTRODUCTION

The development of vaccines based on subunit antigens, recombinant proteins, polysaccharides, or peptide fragments derived from pathogens, has led to increased safety but decreased potency in vaccine candidates compared to that of traditional live attenuated microbe vaccines. To increase the immunogenicity of subunit vaccines, adjuvants play an important role in vaccine development. Adjuvants are materials that enhance immune responses elicited by vaccines either by providing inflammatory signals (e.g., ligands for Toll-like receptors¹), modulating the delivery of antigen to immune cells, or both.² For example, antigen delivery can be altered by providing a depot for long-term antigen release from a vaccination site. Long-term biomolecule release is often achieved by encapsulation of the cargo into a biodegradable polymer matrix, such as poly(lactide-*co*-glycolide) (PLGA), which is often employed because of its history of safe use in humans, efficient encapsulation of hydrophobic materials, and tunable drug release behavior.³ However, delivery of protein antigens encapsulated in PLGA micro- or nanoparticles is challenging because of the low antigen encapsulation efficiency and denaturation/aggregation of proteins during encapsulation and release.^{4–6} Alternatively, antigen delivery can be modulated at the single-cell level by surface-displaying antigens on the surfaces of particulate carriers such as liposomes or polymer

particles. Surface display has been shown to enhance immune responses, likely by increasing the degree of B-cell receptor cross-linking and subsequent B-cell activation.^{7–13} Furthermore, incorporation into lipid particles has been previously shown to be an effective delivery method of lipophilic adjuvants such as MPLA.^{14,15} Despite the disadvantages of degradable polymers for use with protein antigen, these polymers remain attractive for the slow-release co-delivery of inflammatory adjuvant compounds that could shape the immune response over time.^{16–19}

In order to combine the surface display of antigen with a biodegradable core in which we could ultimately co-deliver additional adjuvant molecules, we recently described an approach for synthesis of lipid-enveloped polymer microparticles and nanoparticles that present antigen bound to a surface lipid bilayer.²⁰ A self-assembled lipid bilayer coat surrounding a PLGA core was achieved by using lipids as the surfactant component of an emulsion/solvent evaporation-based PLGA particle synthesis. The lipid bilayer was observed to be a two-dimensionally fluid surface that tightly envelops the polymer core. We employed these lipid-coated microparticles

Received: March 4, 2014

Revised: May 31, 2014

Published: June 4, 2014

(LCMPs) as vaccine delivery agents by conjugating protein antigens to PEGylated lipids anchored in the bilayer coating and co-incorporating adjuvant compounds such as the TLR agonist monophosphoryl lipid A (MPLA) or α -galactosyl ceramide in the particles. LCMPs elicited high, durable humoral immune responses in response to injection of as little as 2.5 ng of the model antigen ovalbumin (OVA) surfaced-displayed on LCMPs.²¹ In addition, these particles triggered antigen-specific proliferation of both CD4⁺ and CD8⁺ T-cells and production of Th1-biased cytokines from T-cells *in vivo*.²¹ When formulated as nanoparticles and functionalized with a candidate malaria antigen VMP0001 and MPLA, lipid-coated particles were shown to induce germinal center formation and elicited higher, more durable antigen-specific titers of IgG antibodies of diverse isotypes compared to those produced by vaccination with soluble VMP001 and MPLA.²²

Despite the efficacious nature of these lipid-coated particles, it was unclear how they presented antigen to the immune system, particularly in the case of LCMPs, because these microparticles (diameter, $2.6 \pm 1.2 \mu\text{m}$) did not freely drain to lymph nodes.²³ However, during initial cryo-TEM characterization studies on the LCMPs, we observed that over time the lipid bilayers at the surface of the biodegradable particles begin to delaminate from the polymer core.²⁰ This observation of delamination suggested that the lipid bilayer might not be stable on the PLGA particle cores over time. Since antigen was conjugated to the lipid bilayer, we hypothesized that delamination of the lipid envelope could play a role in the adjuvant characteristics of LCMPs.

Here, we directly evaluated the stability of the bilayer coating of LCMPs and examined the role of bilayer delamination in the immunogenicity of this particulate vaccine system. We found that under physiological conditions LCMPs exhibit rapid bilayer delamination, leading to the release of antigen-bearing lipid vesicles. We evaluated the kinetics of bilayer shedding and the resulting effects on the immunogenicity of LCMPs *in vivo*. In addition, we explored the kinetic dependence of lipid delamination on the presence of lipid/serum in the surrounding environment. To test the hypothesis that delamination impacts immunogenicity, stabilized-bilayer LCMPs were developed either by the inclusion in the lipid bilayer of cholesterol or lipids with saturated carbon chains. Mice immunized with OVA-LCMPs generated higher anti-OVA titers than mice immunized with stabilized-bilayer OVA-LCMPs or OVA on delaminated lipid vesicles (DLVs) alone. These results suggest that the *in situ* release of delaminated lipid vesicles enhances humoral immune responses to surface-displayed antigen, with LCMPs acting as a source of *in situ* generated antigen-bearing liposomes following injection.

MATERIALS AND METHODS

Materials. All lipids, 1,2-dioleoyl-*sn*-glycero-3-phosphocholine (DOPC), 1,2-dioleoyl-*sn*-glycero-3-phospho-(1'-*rac*-glycerol) (DOPG), 1,2-distearoyl-*sn*-glycero-3-phosphocholine (DSPC), 1,2-distearoyl-*sn*-glycero-3-phosphoethanolamine-*N*-[maleimide(poly(ethylene glycol))2000] (DSPE-PEG2K-maleimide), 1,2-dioleoyl-*sn*-glycero-3-phosphoethanolamine-*N*-(lissamine rhodamine B sulfonyl) (14:0 Liss-Rhod-DOPE), 1,2-distearoyl-*sn*-glycero-3-phosphoethanolamine-*N*-(7-nitro-2-1,3-benzoxadiazol-4-yl) (NBD-DSPE), and cholesterol, were purchased from Avanti Polar Lipids (Alabaster, AL). Poly(lactic-co-glycolic acid) (PLGA) with a 50:50 ratio of lactic acid and glycolic acid and an inherent viscosity of 0.42 dL/G was purchased from Evonik Corporation (Birmingham, AL). Monophosphoryl lipid A (MPLA, from *Salmonella enterica* serotype minnesota Re S95, cat. no.

L6895) and solvents were purchased from Sigma-Aldrich (St. Louis, MO). *N*-Succinimidyl *S*-acetyl(thiotetraethylene glycol) (SAT(PEG)₄) was purchased from Pierce Biotechnology (Rockford, IL). Purified ovalbumin (OVA) was purchased from Worthington Biochemical (Lakewood, NJ) and subsequently passed through detoxi-gel endotoxin-removing columns (Pierce Biotechnology, Rockford, IL) to remove any trace endotoxin.

Synthesis of Lipid-Coated Microparticles (LCMPs). Microparticles consisting of a PLGA core and lipid bilayer envelope were synthesized as previously reported.^{20,24} Briefly, 5 mg of lipid in a 72:18:10 DOPC/DOPG/DSPE-PEG2K-maleimide molar ratio (for DOPC-LCMPs) or a 75:16:9 DSPC/DOPG/DSPE-PEG2K-maleimide molar ratio (for DSPC-LCMPs) was dried under nitrogen followed by incubation under vacuum at 25 °C for 18 h. The resulting lipid film was dissolved in dichloromethane (DCM) containing PLGA for a final polymer/lipid weight ratio of 16:1. This organic solution was emulsified into distilled deionized ultrapure water by homogenization at a ratio of 8:1 aqueous phase/organic phase, stirred for 12 h at 25 °C to remove DCM by evaporation, and passed through a 40 μm filter. Microparticles were isolated from the resulting polydisperse samples by two centrifugation steps at 1100 rcf for 1 min each, with removal of the supernatant and resuspension into pH 7.4 PBS following each centrifugation step. Particle size distributions were determined using the Horiba Partica LA-950 V2 laser diffraction particle size analysis system.

Synthesis of Liposomes. Liposomes prepared with a 72:18:10 molar ratio of DOPC/DOPG/DSPE-PEG2K-maleimide were used for immunization studies, and vesicles with an 80:20 molar ratio of DOPC/DOPG were used for *in vitro* lipid delamination studies. Lipid films dried as described above were resuspended in pH 7.4 PBS, vortexed for 30 s every 10 min for 1 h, subjected to six freeze-thaw cycles in liquid nitrogen and a 37 °C water bath, and extruded for 21 passes through a 200 nm pore polycarbonate membrane (Whatman Inc., Sanford, ME). Vesicle sizes were determined by dynamic light scattering (Brookhaven 90 Plus particle size analyzer, Worcetershire, UK). Liposomes were stored at 4 °C until use.

Antigen Conjugation onto Lipid-Enveloped Particles and Liposomes. Thiolated OVA was conjugated to the surface of maleimide-functionalized lipid-enveloped particles or liposomes as previously described.²⁴ In brief, endotoxin-free OVA was functionalized with the heterobifunctional cross-linker SAT(PEG)₄ (Pierce Biotechnology, Rockford, IL), which was then deacetylated to expose sulfhydryl groups following the manufacturer's instructions. Following buffer exchange into 10 mM EDTA (pH 7.4), via 7000 MWCO Zeba spin desalting columns (Pierce Biotechnology, Rockford, IL), thiolated OVA (5 mg/mL) was incubated with particles (70 mg/mL) or liposomes (3 mg/mL) at 25 °C for 4 h (for particles) or overnight (for liposomes). To remove unbound antigen, particles were washed three times by centrifugation for 5 min at 10 000 rcf with pH 7.4 PBS, and liposomes were washed three times by centrifugation in 30 kDa MWCO Vivaspine columns (Vivaproducts, Littleton, MA). The amount of OVA coupled was determined by solubilizing lipids from the particles/vesicles in 30 mM Triton X-100 and measuring the quantity of OVA by enzyme-linked immunosorbent assay (ELISA). Particles and liposomes were stored at 4 °C until use, which was within 4 h for immunization experiments and 48 h for *in vitro* experiments.

Analysis of Lipid Delamination from LCMPs. Particles were synthesized as described above, incorporating 2 mol % of 14:0 Rhod-DOPE (for DOPC-LCMPs) or NBD-DSPE (for DSPC-LCMPs) in the lipid composition. For characterization of the delamination of protein antigen displayed on the lipid envelope, OVA was conjugated to lipid-enveloped particles as described above. Postsynthesis, particles were washed three times by centrifugation at 5000 rcf for 5 min and subsequent suspension in pH 7.4 PBS. After the third wash, particles were suspended at 12 mg/mL in pH 7.4 PBS, fetal bovine serum, or 10 mM 80:20 DOPC/DOPG liposomes in pH 7.4 PBS, divided into 150 μL aliquots in separate eppendorf tubes for each time point/replicate, and incubated with rotation at 37 °C. At each time point, replicate aliquots were centrifuged for 20 min at 16 100 rcf, and the resulting supernatant was collected for analysis. Lipid release from the LCMPs

was determined by adding 30 mM Triton X-100 to the supernatants, measuring rhod-DOPE fluorescence in a fluorescence plate reader (Tecan Infinite M200 Pro, Männedorf, Switzerland), and normalizing to the total amount of fluorescent lipid present. OVA released from particles was determined by anti-ovalbumin ELISA on the supernatants of the particle aliquots, and the values were normalized to the total amount of OVA–lipid present. This total amount of lipid per aliquot was determined in fluorescently tagged samples by addition of Triton to three or four standard aliquots, which were incubated at 55 °C and subsequently vortexed and sonicated for 1 min each prior to centrifugation for 15 min at 16 100 rcf followed by fluorescent-based quantification of the supernatant. To determine the total amount of the antigen, OVA, released from DOPC–LCMPs particles, the same procedure as above was employed without the 55 °C incubation step and with ELISA-based quantification. The 55 °C incubation step is unnecessary for lipid delamination from DOPC–LCMPs and therefore was omitted to prevent any degradation of the OVA protein.

Size Characterization of Delaminated Lipid Vesicles.

DOPC–LCMPs were prepared and incubated at 37 °C in pH 7.4 PBS for 7 days, after which the microparticles were pelleted via a 30 min centrifugation step at 16 100 rcf. The size distribution of DLVs in the supernatant was determined by laser diffraction as described above.

Animal Studies. All animal experiments were conducted under an IUCAC approved protocol in accordance with local, state, and NIH animal care and use guidelines. Immunizations were carried out on female BALB/c mice, 6 to 7 weeks of age, purchased from Jackson Laboratories. Immediately prior to immunization, 1.3 μg of the TLR-4 agonist, MPLA, per 50 μL was mixed with 10 ng of OVA conjugated to LCMPs, DLVs, or liposomes in sterile pH 7.4 PBS, following postsynthesis insertion techniques described previously.^{21,25} Mice were immunized by injection of 50 μL solutions s.c. at the tail base and were boosted 14 days later. Serum samples were collected on a weekly basis for analysis of serum antibody titers.

Antibody Titer Measurements. Serum total IgG titers, isotype IgG₁ and IgG_{2A} titers, and avidity indices were determined as previously described.²⁴ Briefly, 96-well plates were coated with OVA, blocked with bovine serum albumin, incubated with serially diluted serum, and detected with HRP-labeled antimouse IgG, IgG₁, or IgG_{2A} (Bio-Rad) followed by development and measurement of optical absorbance at 450 nm. Antibody titer is reported as reciprocal serum dilution at an absorbance of 0.5. For avidity indices, duplicate serum dilutions were prepared for each sample, and for one set of dilutions, wells were incubated for 10 min with 6 M urea prior to detection with the respective anti-mouse secondary antibody. The avidity index is reported as the ratio of the titers of the urea-treated sample to those of the non-urea-treated sample.

Statistical Analysis. Statistical analyses were performed using GraphPad Prism software. Comparisons of formulations over time were performed using two-way ANOVA tests, and comparisons of multiple formulations at a single time point were performed using one-way ANOVA tests. Two-tailed unpaired Student *t* tests were used to determine statistical significance between two experimental groups for all other data.

RESULTS AND DISCUSSION

Shedding of Lipid Vesicles from LCMPs. We previously reported that phospholipids incorporated into PLGA particles during an emulsion/solvent evaporation synthesis segregate to the surface of nascent particles, self-assembling into a lipid envelope surrounding the polymer core (Figure 1A). When these particles were incubated in pH 7.4 PBS at 37 °C for 7 days to permit partial hydrolysis of the biodegradable particle core, cryo-TEM imaging revealed evidence of delamination of lipid bilayers from the particle surfaces, which was observed even in the absence of added MPLA, suggesting that adjuvant incorporation did not induce this effect.²⁰ This finding suggested that lipids might be shed from LCMPs by “budding” of lipid bilayers from the particles over time (Figure 1A). This

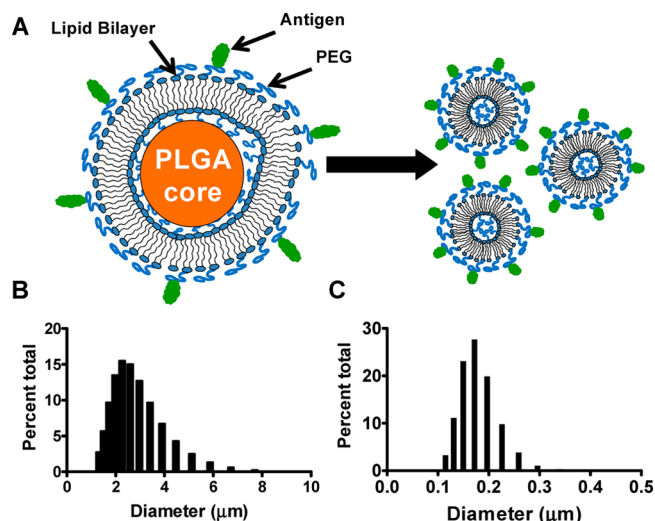


Figure 1. (A) Schematic structure of as-synthesized LCMPs with surface-conjugated protein antigen and vesicles “budded” from PLGA polymer core, forming delaminated-lipid vesicles (DLVs). (B) Size distribution of freshly synthesized microparticles after wash steps determined by laser diffraction. (C) Size distribution of delaminated vesicles released from LCMPs after 7 days in PBS at 37 °C determined by laser diffraction.

might be particularly promoted *in vivo*, as serum albumin and lipoproteins are known to extract lipid from fluid bilayers.^{26–28} To directly test this hypothesis, LCMPs with a diameter of $2.54 \pm 0.95 \mu\text{m}$ (Figure 1B) were incubated in PBS at 37 °C for 1 week. After this incubation time, the PLGA particle cores were still macroscopically intact,²⁰ and the size distribution of the particles recovered by centrifugation was essentially unchanged from that of the starting material (data not shown). However, analysis of the supernatant by laser diffraction to detect released lipid vesicles revealed nanoparticles with a mean size of $176 \pm 6 \text{ nm}$ in the LCMP supernatants (Figure 1C). These particles were not PLGA fragments, as neat PLGA nanoparticles of this size prepared independently were pelleted by the centrifugation step used to remove LCMPs from the supernatants in this experiment. To verify that these nanoparticles in the LCMP supernatant were in fact lipid vesicles, we prepared particles containing a rhodamine-tagged lipid tracer in the bilayer coating. Fluorescence measurements on the supernatant collected from LCMPs incubated 7 days in PBS at 37 °C showed the release of $54 \pm 11\%$ of the total lipid tracer into the supernatant, confirming the release of delaminated lipid vesicles (DLVs) from the microparticles over time.

We next characterized the kinetics of DLV shedding from LCMPs. Microparticles containing rhodamine-labeled lipid were incubated in PBS and DLVs released into the supernatants over time were detected by fluorescence spectroscopy. As shown in Figure 2A, although lipids remained stably associated with LCMPs at 4 °C, vesicles were rapidly shed from the particles at 37 °C in PBS, with delamination reaching a plateau after 24 h. To test the effect of serum on lipid delamination kinetics, LCMPs containing rhodamine-conjugated lipid were incubated in either serum or PBS, and delamination was quantified as before. Figure 2A shows that serum increased the fraction of delaminated lipid by 1.6-fold, with substantial vesicle shedding within 4 h that continued slowly through 48 h. We hypothesized that interactions of the lipid surface layers with lipid droplets in serum may be a major contributor to vesicle

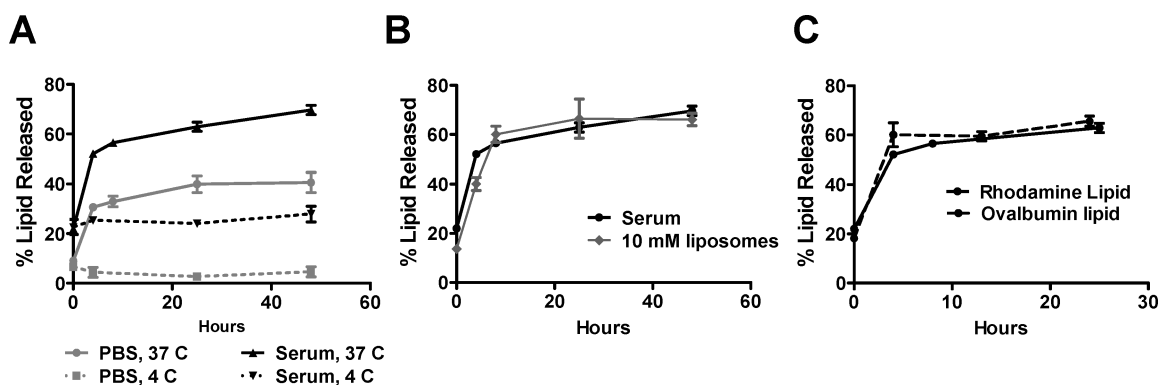


Figure 2. Kinetics of lipid delamination from LCMPs *in vitro* determined by monitoring release of fluorescently labeled lipid tracer (A–C) or PEG-lipid-conjugated OVA (C) into the supernatants of particles over time. (A) Release of rhodamine-lipid into the supernatant of LCMP particles was assessed as a function of temperature in pH 7.4 PBS or 100% fetal bovine serum ($p < 0.0001$ comparing 37 °C serum to 37 °C PBS, 4 °C serum to 4 °C PBS, 37 °C serum to 4 °C serum, and 37 °C PBS to 4 °C PBS). (B) Lipid release kinetics for rhodamine-lipid-labeled LCMPs incubated in PBS containing 10 mM unlabeled DOPC/DOPG liposomes at 37 °C. (C) LCMPs conjugated with OVA protein were incubated in 100% fetal bovine serum at 37 °C, and OVA accumulation in the supernatant was assessed over time by ELISA analysis of LCMP supernatants.

delamination, as the adsorption of lipids by serum lipoprotein particles is essential for lipid transport *in vivo*.²⁹ Previous studies have shown that liposomes are destabilized in the presence of serum because of the transfer of phospholipids to lipoproteins.^{26,27,30} To model interactions of LCMPs with lipids in serum, a group of microparticles was incubated in PBS containing 10 mM of 200 nm diameter synthetic 4:1 DOPC/DOPG liposomes. The results indicate that the inclusion of liposomes in the aqueous buffer replicates the kinetics of lipid delamination in serum (Figure 2B), suggesting that the presence of environmental lipid promotes DLV delamination from LCMPs.

LCMPs carrying protein antigen covalently linked to the membrane (e.g., as illustrated in Figure 1A) elicit robust humoral immune responses *in vivo*.^{22,24} To test whether antigen conjugated to the lipid coat is transferred to delaminating vesicles, thiol-functionalized OVA was conjugated to maleimide-functionalized PEG chains incorporated into the particle bilayer coating, and its release over time into serum at 37 °C was quantified by ELISA. As expected, lipid-conjugated OVA was shed from the LCMPs with kinetics matching rhodamine-labeled lipid delamination (Figure 2C). Altogether, these data suggest that LCMPs rapidly shed submicrometer liposomes under conditions mimicking interstitial fluid to which the particles would be exposed during immunization *in vivo*.

Delaminated Vesicles Prime Antibody Responses Nearly Equivalent to Those of LCMPs. Given the rapid shedding of liposomes from LCMPs in the presence of serum, we hypothesized that vesicles spontaneously released from the microparticles following injection could play an important role in the immunogenicity of LCMP vaccines. To explore this possibility, we prepared OVA-conjugated LCMPs and incubated a fraction of the particles at 37 °C in PBS to induce delamination, followed by collection of the supernatant containing shed vesicles. The concentration of antigen in the shed vesicle preparation was measured by ELISA, and mice were then immunized with MPLA mixed with 10 ng of OVA carried by purified delaminated vesicles or the parent (non-delaminated) particle fraction. In addition, a third group of mice were immunized with OVA-conjugated pure liposomes prepared with the same lipid composition as the LCMPs to control for possible changes in the lipid structure or composition occurring during budding of vesicles from the

PLGA-core particles. Each group of mice was boosted on day 14 with identical formulations, and serum was collected over time for analysis of titers of anti-OVA IgG. As shown in Figure 3A,B, DLVs and the control synthetic liposomes elicited essentially identical OVA-specific IgG responses. Both liposomal vaccines were somewhat less immunogenic than that of intact LCMPs, eliciting average antibody titers 2-fold lower than LCMPs. However, DLVs were still capable of priming a strong immune response to this low dose of OVA, which

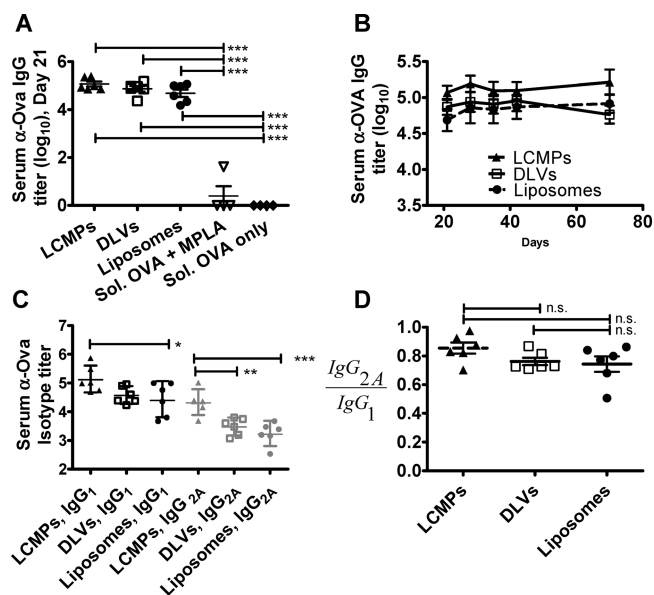


Figure 3. (A–D) BALB/c mice ($n = 6$ /group) were immunized s.c. with 10 ng of OVA displayed on lipid-enveloped microparticles (LCMPs), delaminated lipid vesicles (DLVs) collected from LCMPs, or pure liposomes and were boosted with identical formulations on day 14. Liposomal vaccines are compared to control immunizations with soluble OVA. In all particle formulations, 1.3 μ g of MPLA per injection was included. (A) Mean end-point OVA-specific IgG serum titers on day 21 (***, $p < 0.001$). (B) Mean end-point OVA-specific IgG serum titers over time ($p = 0.006$ for formulation over time). (C) OVA-specific IgG₁ and IgG_{2A} isotype serum titers at day 21 (*, $p < 0.05$; **, $p < 0.01$; ***, $p < 0.001$). (D) Ratio of post boost peak (day 28) end-point OVA-specific IgG_{2A} to IgG₁ serum titers.

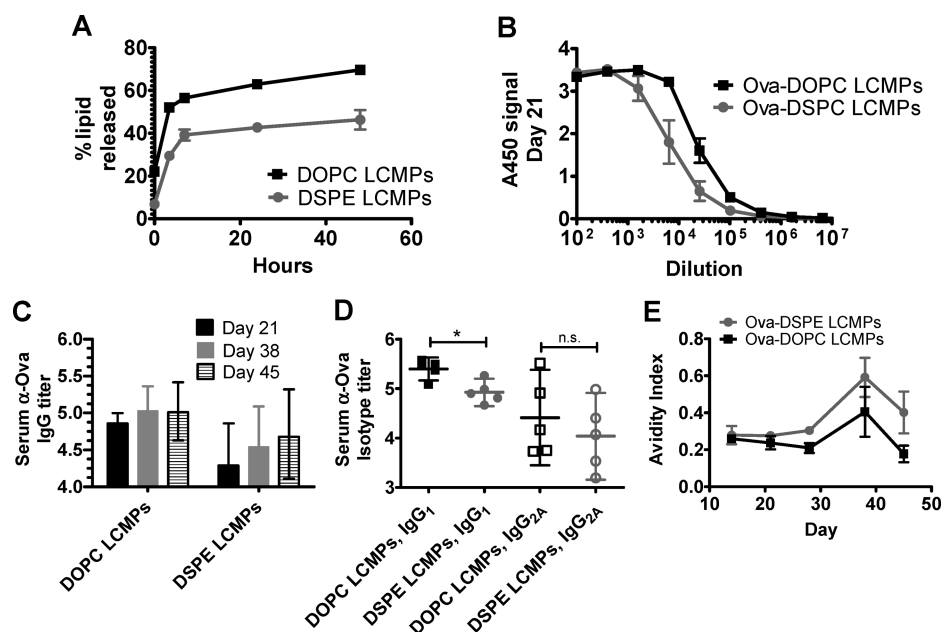


Figure 4. LCMPs prepared with high- T_M lipids show reduced vesicle shedding and weaker antibody responses *in vivo*. (A) Kinetics of *in vitro* lipid release from high- T_M lipid-enveloped microparticles (DSPC-LCMPs) or regular, low- T_M lipid microparticles (DOPC-LCMPs) in serum, determined by following fluorescent lipid tracer released into particle supernatants upon incubation with FBS at 37 °C ($p < 0.0001$). (B–E) BALB/c mice ($n = 5$) were immunized on days 0 and 14 with 1.3 μg of MPLA mixed with DOPC-LCMPs or DSPC-LCMPs, each conjugated with 10 ng of OVA. (B) OVA-specific antibodies detected by ELISA as a function of serum dilution at the post boost peak, day 21 ($p < 0.0001$). (C) Mean OVA-specific IgG serum titers on days 21, 38, and 45 (DOPC-LCMPs vs DSPC-LCMPs over time, $p = 0.0023$). (D) OVA-specific IgG₁ and IgG_{2A} isotype serum titers at day 21 (DOPC IgG₁ vs DSPC IgG₁, *, $p = 0.0067$). (E) Mean OVA-specific IgG avidity indices as a function of time ($p = 0.0491$).

elicited undetectable anti-OVA titers in three out of four animals when administered as a soluble vaccine mixed with MPLA (Figure 3A). Titers in all three particle immunization groups were maintained over at least 70 days post priming. Although DLVs elicited weaker OVA-specific IgG₁ and IgG_{2A} antibodies than those elicited by parent LCMPs (Figure 3C), both groups exhibited identical IgG_{2A}/IgG₁ ratios (Figure 3D). As IgG_{2A} is considered to be indicative of “Th1-like” responses and IgG₁, “Th2-like” responses, this result suggests both the lipid-coated microparticles and shed liposomes primed balanced Th1/Th2 responses and that the small difference in titers comparing LCMPs and shed vesicles reflects a difference in strength of priming rather than different Th-biasing of the antibody response. Altogether, these data suggest that delamination of antigen-bearing liposomes plays a critical role in the immune response primed by LCMPs carrying surface-bound antigens.

Immunogenicity of Stabilized-Envelope LCMPs.

Although Figure 3 demonstrates that *in vitro* generated DLVs induced slightly lower antibody titers than those by parental LCMPs, it remained unclear whether *in vivo* budding of antigen-carrying vesicles from the microparticles was necessary for the high immunogenicity of the lipid-coated microparticles. If *in vivo* delamination were essential, then LCMPs that failed to undergo lipid delamination would be expected to prime weaker immune responses. To test this hypothesis, we sought to prepare LCMPs with lipid envelopes stabilized against delamination. We tested two strategies to create such stabilized-envelope particles: incorporation of high- T_M lipid and incorporation of cholesterol into the lipid coating.

Phospholipids with high melting temperatures have few/no unsaturated bonds in their acyl tails, allowing the lipids to pack

tightly and favoring formation of liquid crystalline gel phases. In addition, the removal of double bonds in the acyl chains of phospholipids in vesicles reduces the rates of lipid transfer from liposomes to serum lipoproteins by 4-fold.³¹ Therefore, DSPC ($T_M = 55$ °C) was used in place of DOPC ($T_M = -20$ °C) to generate high- T_M DSPC-LCMPs. *In vitro*, inclusion of high- T_M lipid did not block vesicle shedding completely but did lower the fraction of lipid lost from the particles in the presence of serum by 33%, as shown in Figure 4A. We tested whether the reduced shedding of vesicles would impact the immunogenicity of these particles compared to that of DOPC-based LCMPs. BALB/c mice were immunized s.c. on days 0 and 14 with MPLA mixed with DOPC-LCMPs or DSPC-LCMPs each carrying 10 ng of OVA. As shown in Figure 4B, despite the modest reduction in lipid shedding exhibited by DSPC-LCMPs, the immunogenicity of these particles was significantly altered, as mice immunized with DSPC-LCMPs showed a 3.5-fold reduction in titers of OVA-specific antibodies compared to those from DOPC-LCMPs at 1 week post boost (Figure 4B). Furthermore, DSPC-LCMPs elicited $64 \pm 10\%$ lower total OVA-specific IgG titers ($p = 0.0023$, Figure 4C) and lower serum IgG₁ titers at the post boost peak on day 21 ($p = 0.0067$, Figure 4D) when compared to those of DOPC-LCMPs. Interestingly, the avidity index of the antibody response elicited by DSPC-LCMPs was higher than that of the response primed by to DOPC-LCMPs from day 28 onward ($p = 0.0491$ comparing the two groups over time). However, the overall strength of the antibody response elicited by LCMPs was reduced when vesicle shedding was impeded by incorporation of high- T_M lipids.

To further test the idea that vesicle budding from antigen-conjugated LCMPs is important for their immunogenicity, we

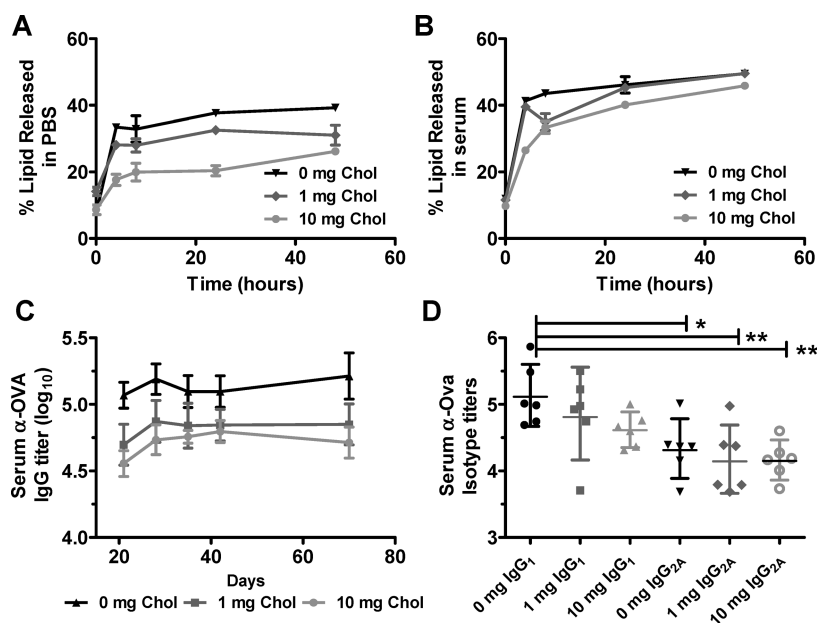


Figure 5. Cholesterol was included in the lipid bilayer of LCMPs to decrease delamination of the envelope. (A, B) Kinetics of lipid release, in PBS (A) or fetal bovine serum (B), of LCMPs, which were synthesized with 0, 1, or 10 mg of cholesterol (per standard 80 mg PLGA batch). Delamination was quantified by the fluorescent detection of rhodamine-lipid in the supernatant of aliquots of pelleted microparticles. (A: $p < 0.0001$; B: $p < 0.0001$ for effect of cholesterol over time.) (C, D) BALB/c mice ($n = 5$) were immunized and boosted 14 days later with 10 ng of OVA conjugated to the surface of LCMPs containing 0, 1, or 10 mg of cholesterol per batch. In all formulations, 1.3 μ g of MPLA per mouse was incorporated into the lipid bilayer. (C) Mean end-point ELISA-based OVA-specific IgG serum titers over time (comparison of 10 vs 1 mg titer over time, $p < 0.0001$). (D) End-point OVA-specific IgG₁ and IgG_{2A} isotype serum titers at day 28, the post boost peak (*, $p < 0.05$; **, $p < 0.01$).

also tested a second strategy for inhibiting liposome shedding from the microparticles. Cholesterol is a major component of cell membranes and is often used as a stabilizing agent in lipid vesicle preparations because it orders and condenses fluid-phase bilayers.^{32–34} Thus, we hypothesized that cholesterol, like high- T_M lipids, could also act to stabilize the lipid bilayer of LCMPs. We prepared DOPC–LCMPs incorporating 0, 1, or 10 mg of cholesterol per 80 mg of PLGA. *In vitro*, DLV formation was not inhibited completely by the inclusion of cholesterol, but delamination did decrease with increasing cholesterol quantity. As shown in Figure 5A,B, increasing the amount of cholesterol incorporated in the particles lowered the fraction of lipid shed into solution from LCMPs, although the effect was less pronounced in serum than in PBS, perhaps because of cholesterol absorption by lipoprotein particles in serum. As with the high- T_M lipid LCMPs, we tested the immunogenicity of LCMPs with cholesterol by vaccinating BALB/c mice. A plot of mean OVA-specific IgG end-point titers shows decreased immunogenicity (up to a 2.5-fold average drop in titers) with increasing cholesterol content (Figure 5C) (comparison of 10 vs 1 mg titer over time, $p < 0.001$). An analysis of IgG₁ and IgG_{2A} isotype titers at the post boost peak indicates that IgG₁ titers are also inversely dependent on cholesterol quantity; however, IgG_{2A} isotype titers remained relatively independent of cholesterol presence (Figure 5D). Interestingly, avidity indices were independent of cholesterol incorporation in the particles (data not shown). Thus, using a second strategy to stabilize the lipid bilayer of LCMPs by altering its composition, we found a similar reduction in antibody responses when vesicle shedding was inhibited.

The agreement in results obtained by these two different strategies for physically stabilizing the bilayer suggests that the reduced immunogenicity observed with DSPC–LCMPs or chol/DOPC–LCMPs when compared to that with DOPC–

LCMPs is not due to the chemical alterations in the bilayer composition. The antibody response to LCMPs was not entirely ablated by inhibiting vesicle delamination, but the reduced response is all the more striking given the fact that the lipid bilayer composition-based strategies we tested here for blocking DLV release from the particles were at best only ~30% effective under conditions mimicking exposure to serum components. Furthermore, the immunogenicity of liposomes is inversely proportional to membrane fluidity, and it has been specifically shown that inclusion of cholesterol or high- T_M lipid in liposome vaccine formulations increases immunogenicity.³⁵ Thus, an enhancement derived from decreased membrane fluidity of shedded liposomes may be masking the full impact that decreased delamination from LCMPs has on humoral antibody responses. Altogether, these results are consistent with vesicle shedding from LCMPs playing an important role in the priming of humoral responses by these microparticle vaccines. An advantage of this system is the 180 nm diameter of DLVs, as nanoparticles in this size range are well-suited for delivery to lymph nodes via subcutaneous injection and direct draining into the lymphatic system.³⁶ Furthermore, antigen that drains freely to lymph nodes can interact directly with B-cells, which generates optimal humoral immune responses.³⁷

Coupling the observed reduction in immunogenicity from lipid-stabilized LCMPs with the *in vitro* observation of identical delamination kinetics of LCMPs in serum or in 10 mM liposome buffer leads to the possibility that antigen conjugated to lipid on LCMPs may be taken up by lipoprotein particles *in vivo*. This uptake and subsequent circulation throughout the lymphatic system could account for the enhanced immunogenicity of LCMPs over stabilized-lipid bilayer MPs or synthetic liposomes. Prior work characterizing the lipid transfer between liposomes and lipoproteins further supports this concept, especially as inclusion of cholesterol in liposome formulations

was shown to decrease the rate of lipid transfer to lipoproteins.³⁰ These results are consistent with our observation of decreased immunogenicity of LCMPs with increasing cholesterol inclusion.

CONCLUSIONS

Here, we have explored the mechanisms underlying the potent immunogenicity of lipid-coated biodegradable microparticles in vaccine delivery. We found that although these particles are too large to efficiently drain from subcutaneous injection sites to lymph nodes, they are still very effective in antigen delivery because of the spontaneous shedding of antigen-bearing lipid vesicles from the particle surfaces, which occurs rapidly under physiological conditions. Changes in lipid composition that reduce microparticle surface vesicle budding lowered the immunogenicity of the particles *in vivo*, suggesting that this mechanism is important for the effectiveness of these antigen delivery vehicles. This antigen-bearing vesicle release combined with molecular adjuvants either incorporated in the membranes (as shown here) or encapsulated in the PLGA particle core and slow-released at the injection site to drain to local lymph nodes^{16–19} could provide an effective strategy for enhancing the immunogenicity of subunit vaccines.

AUTHOR INFORMATION

Corresponding Author

*E-mail: djirvine@mit.edu.

Author Contributions

The manuscript was written through contributions of all authors. All authors have given approval to the final version of the manuscript.

Notes

The authors declare no competing financial interest.

ACKNOWLEDGMENTS

This work was supported in part by the NIH (AI091693), the Gates Foundation, and the Ragon Institute of MIT, MGH, and Harvard. D.J.I. is an investigator of the Howard Hughes Medical Institute.

REFERENCES

- (1) Kanzler, H.; Barrat, F. J.; Hessel, E. M.; Coffman, R. L. *Nat. Med.* **2007**, *13*, 552–559.
- (2) Guy, B. *Nat. Rev. Microbiol.* **2007**, *5*, 505–517.
- (3) Fredenberg, S.; Wahlgren, M.; Reslow, M.; Axelsson, A. *Int. J. Pharm.* **2011**, *415*, 34–52.
- (4) Jiang, W.; Gupta, R. K.; Deshpande, M. C.; Schwendeman, S. P. *Adv. Drug Delivery Rev.* **2005**, *57*, 391–410.
- (5) Gupta, R.; Singh, M.; O'Hagan, D. *Adv. Drug Delivery Rev.* **1998**, *32*, 225–246.
- (6) Fu, K.; Pack, D. W.; Klivanov, A. M.; Langer, R. *Pharm. Res.* **2000**, *17*, 100–106.
- (7) Ghasparian, A.; Riedel, T.; Koomullil, J.; Moehle, K.; Gorba, C.; Svergun, D. I.; Perriman, A. W.; Mann, S.; Tamborrini, M.; Pluschke, G.; Robinson, J. A. *ChemBioChem* **2011**, *12*, 100–109.
- (8) Watson, D. S.; Platt, V. M.; Cao, L.; Venditto, V. J.; Szoka, F. C. *Clin. Vaccine Immunol.* **2011**, *18*, 289–297.
- (9) Hoffmann, P. R.; Kench, J. A.; Vondracek, A.; Kruk, E.; Daleke, D. L.; Jordan, M.; Marrack, P.; Henson, P. M.; Fadok, V. A. *J. Immunol.* **2005**, *174*, 1393–1404.
- (10) Pihlgren, M.; Silva, A. B.; Madani, R.; Giriens, V.; Waeckerle-Men, Y.; Fettelschoss, A.; Hickman, D. T.; López-Deber, M. P.; Ndao, D. M.; Vukicevic, M.; Buccarello, A. L.; Gafner, V.; Chuard, N.; Reis,

P.; Piorkowska, K.; Pfeifer, A.; Kündig, T. M.; Muhs, A.; Johansen, P. *Blood* **2013**, *121*, 85–94.

(11) Taneichi, M.; Ishida, H.; Kajino, K.; Ogasawara, K.; Tanaka, Y.; Kasai, M.; Mori, M.; Nishida, M.; Yamamura, H.; Mizuguchi, J.; Uchida, T. *J. Immunol.* **2006**, *177*, 2324–2330.

(12) Fifis, T.; Gamvrellis, A.; Crimeen-Irwin, B.; Pietersz, G. A.; Li, J.; Mottram, P. L.; McKenzie, I. F. C.; Plebanski, M. *J. Immunol.* **2004**, *173*, 3148–3154.

(13) de Titta, A.; Ballester, M.; Julier, Z.; Nembrini, C.; Jeanbart, L.; van der Vlies, A. J. *Proc. Natl. Acad. Sci. U.S.A.* **2013**, *110*, 19902–19907.

(14) Richards, R. L.; Rao, M.; Wassef, N. M.; Glenn, G. M.; Rothwell, S. W.; Alving, C. R. *Infect. Immun.* **1998**, *66*, 2859–2865.

(15) Tamauchi, H.; Tadakuma, T.; Yasuda, T.; Tsumita, T.; Saito, K. *Immunology* **1983**, *50*, 605–612.

(16) Jewell, C. M.; López, S. C. B.; Irvine, D. J. *Proc. Natl. Acad. Sci. U.S.A.* **2011**, *108*, 15745–15750.

(17) Westwood, A.; Elvin, S. J.; Healey, G. D.; Williamson, E. D.; Eyles, J. E. *Vaccine* **2006**, *24*, 1736–1743.

(18) Schlosser, E.; Mueller, M.; Fischer, S.; Basta, S.; Busch, D. H.; Gander, B.; Groettrup, M. *Vaccine* **2008**, *26*, 1626–1637.

(19) Jain, S.; O'Hagan, D. T.; Singh, M. *Expert Rev. Vaccines* **2011**, *10*, 1731–1742.

(20) Bershteyn, A.; Chaparro, J.; Yau, R.; Kim, M.; Reinherz, E.; Ferreira-Moita, L.; Irvine, D. J. *Soft Matter* **2008**, *4*, 1787–1791.

(21) Bershteyn, A.; Hanson, M. C.; Crespo, M. P.; Moon, J. J.; Li, A. V.; Suh, H.; Irvine, D. J. *J. Controlled Release* **2012**, *157*, 354–365.

(22) Moon, J.; Suh, H.; Polhemus, M. E.; Ockenhouse, C. F.; Yadava, A.; Irvine, D. J. *PLoS One* **2012**, *7*, e31472.

(23) Bershteyn, A. *Lipid-Coated Micro- and Nanoparticles as a Biomimetic Vaccine Delivery Platform*. Ph.D. Thesis, Massachusetts Institute of Technology, 2010; pp 1–164.

(24) Bershteyn, A.; Hanson, M. C.; Crespo, M. P.; Irvine, D. J. *J. Controlled Release* **2011**, *157*, 354–365.

(25) Iden, D. L.; Allen, T. M. *Biochim. Biophys. Acta, Biomembr.* **2001**, *1513*, 207–216.

(26) Damen, J. A. N.; Regts, J.; Scherphof, G. *Biochim. Biophys. Acta* **1981**, *665*, 538–545.

(27) Allen, T. M. *Biochim. Biophys. Acta* **1981**, *640*, 385–397.

(28) Zborowski, J.; Roerdink, F.; Scherphof, G. *Biochim. Biophys. Acta* **1977**, *497*, 183–191.

(29) Phillips, M. C.; Johnson, W. J.; Rothblat, G. H. *Biochemistry* **1987**, *906*, 223–276.

(30) Kirby, C.; Clarke, J.; Gregoriadis, G. *FEBS Lett.* **1980**, *111*.

(31) Massey, J. B.; Gotto, A. M.; Pownall, H. J. *Biochemistry* **1982**, *21*, 3630–3636.

(32) Kirby, C.; Clarke, J.; Gregoriadis, G. *Biochem. J.* **1980**, *186*, 591–598.

(33) Silviu, J. *Biochim. Biophys. Acta, Biomembr.* **2003**, *1610*, 174–183.

(34) Karmakar, S.; Sarangi, B. R.; Raghunathan, V. A. *Solid State Commun.* **2006**, *139*, 630–634.

(35) Watson, D. S.; Endsley, A. N.; Huang, L. *Vaccine* **2012**, *30*, 2256–2272.

(36) Manolova, V.; Flace, A.; Bauer, M.; Schwarz, K.; Saudan, P.; Bachmann, M. F. *Eur. J. Immunol.* **2008**, *38*, 1404–1413.

(37) Bachmann, M. F.; Jennings, G. T. *Nat. Rev. Immunol.* **2010**, *10*, 787–796.